Role of measurement voltage on hysteresis loop shape in Piezoresponse Force Microscopy

E. Strelcov, Y. Kim, J. C. Yang, Y. H. Chu, P. Yu, X. Lu, S. Jesse, and S. V. Kalinin

---

Articles you may be interested in

Top electrode size effect on hysteresis loops in piezoresponse force microscopy of Pb(Zr,Ti)O3-film on silicon structures
J. Appl. Phys. **112**, 052015 (2012); 10.1063/1.4746028

Piezoresponse force microscopy studies on the domain structures and local switching behavior of Pb(In1/2Nb1/2)O3-Pb(Mg1/3Nb2/3)O3-PbTiO3 single crystals
J. Appl. Phys. **112**, 052006 (2012); 10.1063/1.4745979

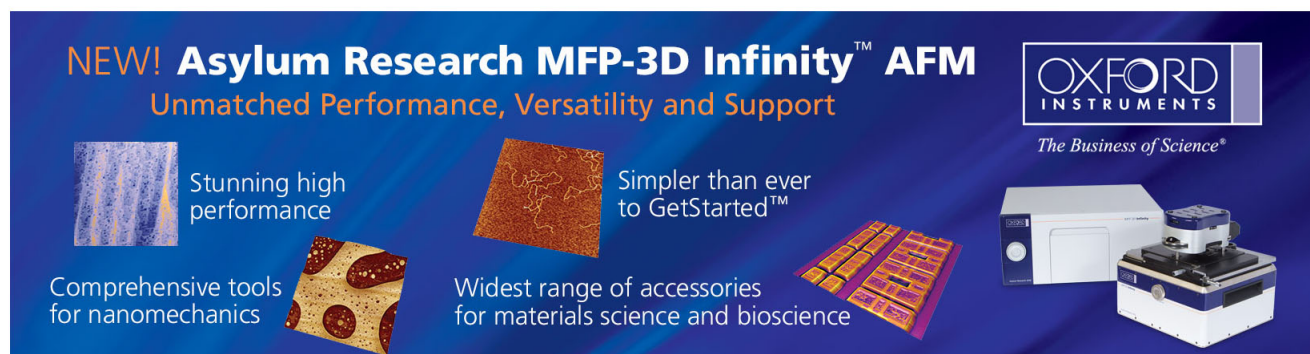Ferroelectric domain structure of PbZr0.35Ti0.65O3 single crystals by piezoresponse force microscopy
J. Appl. Phys. **110**, 052003 (2011); 10.1063/1.3623768

Landau-Ginzburg-Devonshire theory for electromechanical hysteresis loop formation in piezoresponse force microscopy of thin films
J. Appl. Phys. **110**, 052011 (2011); 10.1063/1.3623763

Domain nucleation and hysteresis loop shape in piezoresponse force spectroscopy
Appl. Phys. Lett. **89**, 192901 (2006); 10.1063/1.2378526

Role of measurement voltage on hysteresis loop shape in Piezoresponse Force Microscopy

E. Strelcov,[1] Y. Kim,[1] J. C. Yang,[2] Y. H. Chu,[2] P. Yu,[3] X. Lu,[4] S. Jesse,[1] and S. V. Kalinin[1,a)]

[1]*The Center for Nanophase Materials Sciences, Oak Ridge National Laboratory, Oak Ridge, Tennessee 37831, USA*
[2]*Department of Materials Science and Engineering, National Chiao Tung University, Hsinchu 30010, Taiwan*
[3]*University of California at Berkeley, Department of Physics, Berkeley, California 94720-7300, USA*
[4]*State Key Discipline Laboratory of Wide Band Gap Semiconductor Technology, Xidian University, 710071 Xi'an, China*

The dependence of field-on and field-off hysteresis loop shape in Piezoresponse Force Microscopy (PFM) on driving voltage, V_{ac}, is explored. A nontrivial dependence of hysteresis loop parameters on measurement conditions is observed. The strategies to distinguish between paraelectric and ferroelectric states with small coercive bias and separate reversible hysteretic and non-hysteretic behaviors are suggested. Generally, measurement of loop evolution with V_{ac} is a necessary step to establish the veracity of PFM hysteresis measurements. © *2012 American Institute of Physics.*
[http://dx.doi.org/10.1063/1.4764939]

Hysteresis loop measurements in Piezoresponse Force Microscopy (Piezoresponse Force Spectroscopy, PFS) have emerged as a powerful tool for probing polarization switching in nanoscale volumes.[1–3] In PFS, a slow (1–10 s), large amplitude bias sweep applied to the scanning probe microscopy tip in contact with the surface induces the nucleation and growth of a ferroelectric domain below the tip. A simultaneously measured high-frequency (10 kHz–3 MHz) dynamic response to the small amplitude bias voltage provides information on the degree of switching. The resultant hysteresis loop provides local information on the kinetics and thermodynamics of tip-induced switching and can be analyzed similarly to macroscopic hysteresis loops. The presence of imprint bias or vertical loop shift has been used to analyze the ferroelectric behavior of ferroelectric nanostructures.[4–6] The introduction of spectroscopic imaging modes based on rapid hysteresis loop measurements[7] or stroboscopic imaging at different biases[8–12] has enabled fundamental studies of domain nucleation and growth processes. In certain cases, polarization switching mechanisms were resolved on the level of single structural defects.[13,14]

Despite multiple experimental studies of polarization dynamics using Piezoresponse Force Microscopy (PFM) voltage spectroscopy (local hysteresis loop measurements), the factors affecting the measured response are not well understood. The dominant among these is the role of driving voltage, V_{ac}, on the hysteresis loop shape. Indeed, the measured signal in PFM is directly proportional to V_{ac} and hence large biases improve the signal to noise ratio. At the same time, the high frequency voltage can be expected to affect polarization switching induced by the slow switching waveform. Note that similar studies in the context of other voltage modulated techniques such as Kelvin Probe Force Microscopy have revealed nontrivial insights into the microscope operation and role of topography and topographic cross-talk.[15–17]

In PFM, the role of driving voltage is directly linked to the fundamental dynamics of polarization switching. If domain switching is slow, as limited by, e.g., strong pinning in the bulk or surface screening charge dynamics, the high frequency signal will not significantly affect the hysteresis loop measurements. In the opposite limit, the switching and probing waveforms will result in polarization dynamics equally. The hysteresis loop shape will hence be strongly affected by these relaxation processes. This behavior is particularly of interest in the context of recent work on ultrathin (below 3–10 nm) ferroelectric films[18,19] in which the intrinsic switching biases can be comparable to ~1 V.

To explore these effects systematically, we studied domain switching using band-excitation PFM (BE-PFM)[20,21] implemented on Asylum Research Cypher platforms. For each pixel (locus) of the surface, a bipolar triangular waveform is applied to the tip. The waveform consists of the field-on and field-off DC (direct current) steps, during which AC (alternating current) driving voltage is applied and hysteresis loops are collected (see Figure 1(a)). The typical parameters we used were: bandwidth of 80 kHz, central frequency *ca.* 300 kHz, frequency interval *ca.* 19.5 Hz, the bias sweep rate *ca.* 50 V/s, the sampling rate was 4 MHz. As a first model system, we have chosen a nanocapacitor sample formed by (001) $Pb(Zr_{0.2}Ti_{0.8})O_3$ (PZT) film, which was grown epitaxially by pulsed lased deposition on top of a (001) $SrRuO_3/SrTiO_3$ (SRO/STO) heterostructure (Fig. 1(b)). The SRO film acts as a bottom electrode, the role of the top electrode is played by Au/Cu nanocaps fabricated on the PZT via anodic aluminum oxide masks using an electron beam.[22,23] The large surface area (relative to that of the PFM tip) of the Au/Cu nanocaps ensures uniformity of the electric field in the PZT film and, hence, enhances switching behavior of the system. To ensure statistical averaging, the BE-PFM measurements were performed over 180×180 nm^2 regions centered at the Au/Cu caps each constituting a 3×3 grid of nine spatial locations (Fig. 1(c)). The piezoresponse (PR) signal was averaged over the grid and normalized to the

a)Author to whom correspondence should be addressed. Electronic mail: sergei2@ornl.gov.
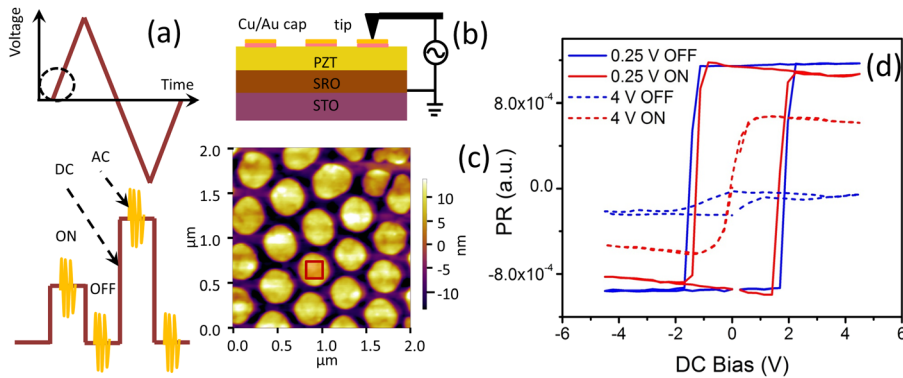
FIG. 1. (a) Voltage waveform applied to the tip: overall (top) and zoomed-up area (bottom). Field on and off measuring states are shown. (b) Schematics of nanoscale capacitor and measurement setup. (c) Topographic map of capacitor sample with location of one of the 180-by-180 nm measurement regions highlighted in red, (d) Piezoresponse (PR) hysteresis loops averaged over a 3×3 (180×180 nm^2) grid. Shown are loops measured in the on and off states at 0.25 V and 4 V driving biases.

AC driving voltage. Little variation has been seen in the switching behavior between different nanocaps except those with some defects and shape deformations (which are not considered below).

The typical hysteresis loops for the caps are shown in Fig. 1(d) and demonstrate an almost ideal rectangular shape for small biases (in previous studies[24] the switching parameters were found to be uniform with respect to the probing position relative to the nanocap center). For field-on *vs.* field-off loops, note the presence of a (small) linear slope (the field-on PR baseline is tilted relative to that of the field-off), presumably due to electrostatic cantilever-surface interactions.[25–27] The increase in AC driving voltage from 0.25 V to 4 V results in drastic changes in the hysteresis loops shape, as illustrated in detail in Figure 2. The field-off loops become progressively narrower with increasing V_{ac}, while the height remains almost constant for low voltages. The coercive and nucleation biases (which coincide for a rectangular loop) are *approximately* 1.5 V for 0.25 V_{ac}, and the loop width decreases almost linearly with the slope close to unity as a function of V_{ac} both for field-on and field-off loops. We further refer to the values of these parameters extrapolated to zero driving voltage as **static**. This observation suggests that for this system the driving voltage and switching voltage

affect polarization dynamics equally regardless of the 5 orders of magnitude difference in frequencies.

The remarkable difference between field-on and field-off loop behavior is observed when driving voltage exceeds the static coercive bias. For the field-off measurements, the hysteresis loop collapses and exhibits only weak residual hysteresis. This behavior can be easily rationalized by the fact that under these conditions the material is switching within the measurement cycle and hence static hysteresis is effectively zero.

The behavior of the field-on loop is surprisingly different. For high biases, the loop narrows down and becomes reminiscent of that for the superparaelectric state. We ascribe this behavior to the fact that in the field-on state the average (over measurement cycle) polarization in the system is maintained by the (small) DC bias.

We note that the observed bias dependence of the loop shape is non-universal. Shown in Figure 3 is the bias evolution of a hysteresis loop measured on 50 nm, monodomain PZT film grown on a SrRuO$_3$/SrTiO$_3$ (001) substrate (no top electrode used). Here, BE-PFM data were collected from 100 points on a 10×10 grid (1.5×1.5 μm^2) and the obtained piezoresponse was averaged and normalized by V_{ac}. In this case, the field-off loops exhibit the classical shape, Figure
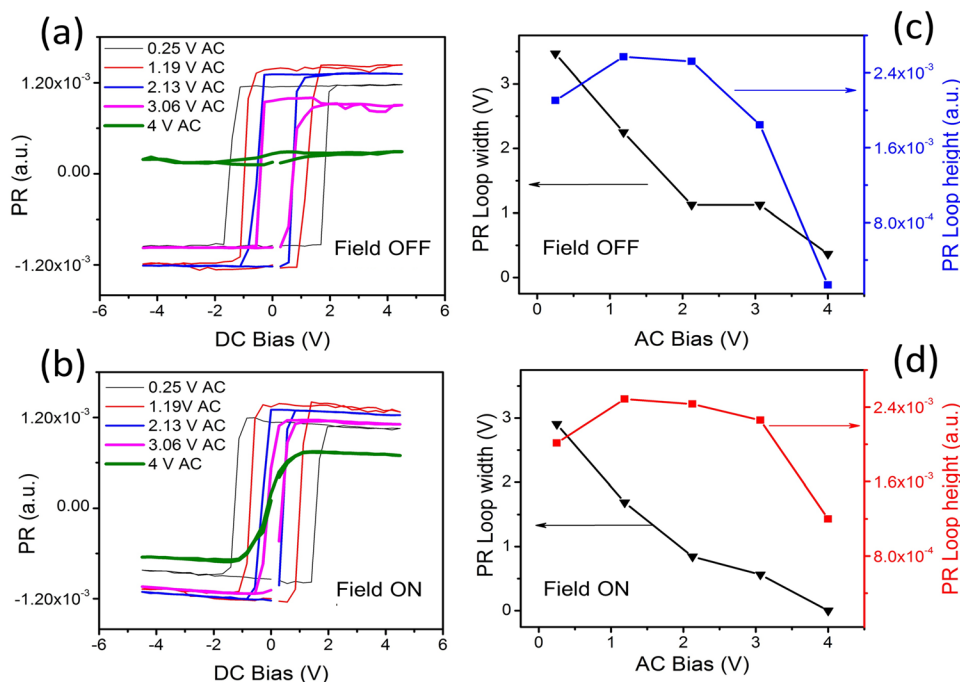

FIG. 2. Evolution of piezoresponse hysteresis loops in nanocapacitors with increasing AC driving voltage for (a) field-off and (b) field-on states. Bias dependence of the effective hysteresis loop parameters for field-off (c) and field-on (d) loops.
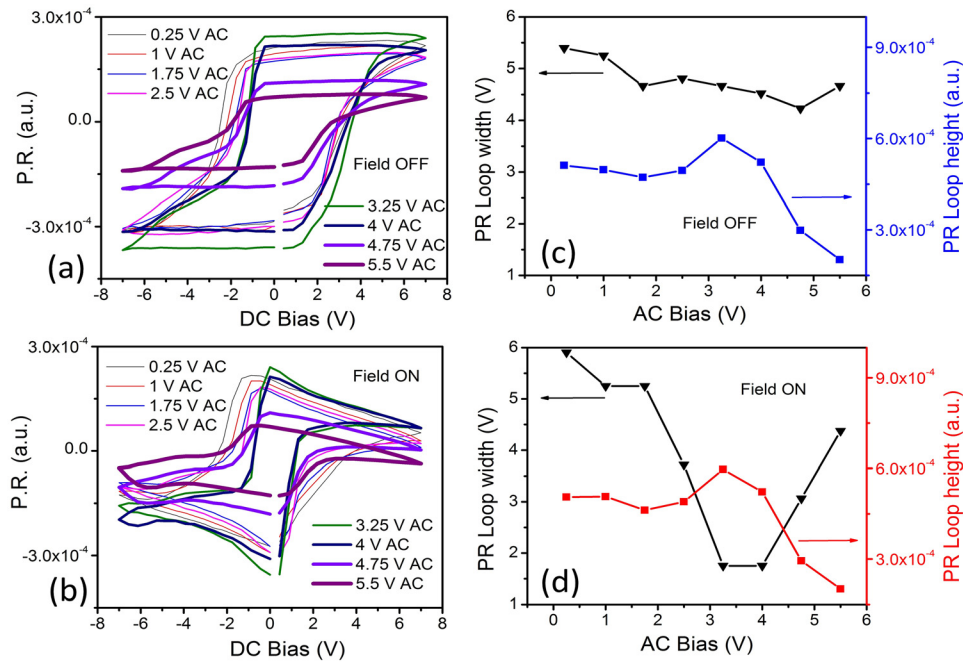
FIG. 3. Normalized piezoresponse hysteresis loop averaged over 10×10 ($1.5 \times 1.5 \, \mu m^2$) grid for PZT thin film. Shown are (a) field-off and (b) field-on loops for different driving biases and (c), (d) loop height and width *vs.* driving bias.

3(a). An increase of the driving voltage above 3 V leads to reduction of the height of the loops, while the corresponding width remains almost constant (Fig. 3(c)). In comparison (Fig. 3(b)), the field-on loops show anomalous (but reproducible across all locations and driving voltages) shape. Their aspect ratio keeps increasing up to 3 V of driving bias due to narrowing, after which the loops significantly widen while simultaneously collapsing in height (Fig. 3(d)). The use of the driving voltage beyond 5.5 V brings about topological changes and the formation of 50-100 nm hillocks at some locations on the grid, suggesting the onset of irreversible electrochemical transformations.[28] This process is associated with the emergence of a wide "tail" at negative DC biases. Thus, the sharp difference in the field-on loop shapes below

and above 4 V of driving bias is due not to the specific aspects of polarization switching but should rather be attributed to partial decomposition of the PZT film.

A much more complicated behavior is observed when a complex ferroelectric-ferroelastic domain structure is present. One such case is shown in Figure 4 for the bias evolution of hysteresis loops measured on 200 nm $BiFeO_3$ films grown on a $SrRuO_3/DyScO_3$ substrate (no top electrode used). These films have characteristically dense 71° wall structures and hence combine ferroelectric and ferroelastic behavior.

At driving voltages less than 3.25 V the field-off piezoresponse is stable, between 3.25 and 4 V loops start to collapse, and above 4 V the film degrades. Field-on loops, although being very anomalous in shape, show similar
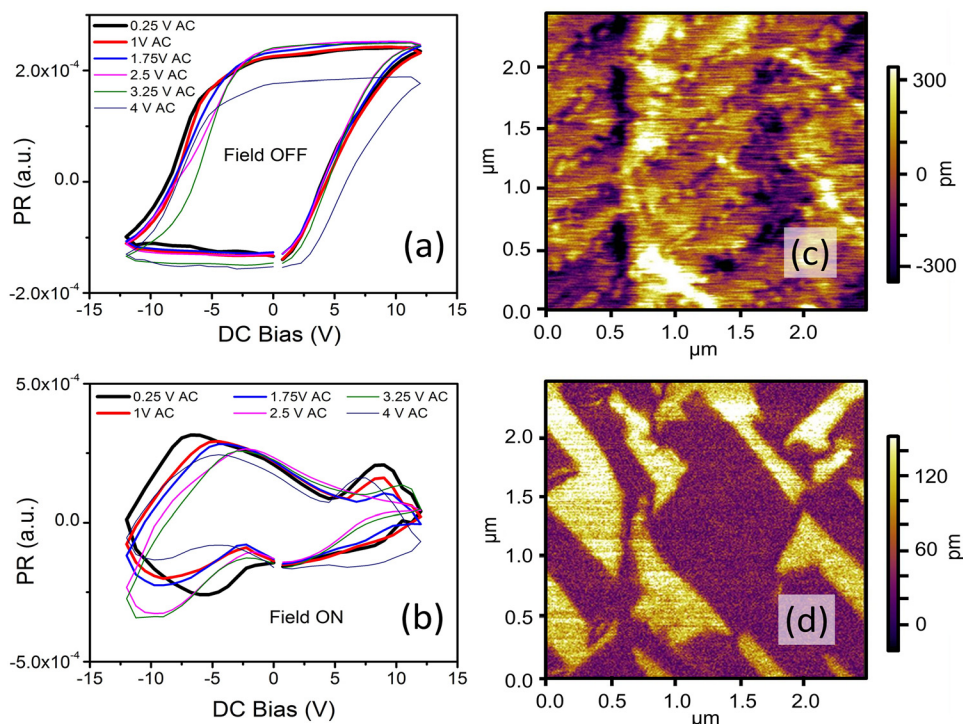

FIG. 4. $BiFeO_3$ sample: Piezoresponse loops for field-off (a) and -on (b) states recorded on a 10×10 ($2 \times 2 \, \mu m$) grid, (c) typical topography of the sample, and (d) in-plane domain structure.

changes. A possible explanation of this behavior may be activation of non-hysteretic ferroelastic polarization switching, including wall twists.[29–31] The field-off loop behavior is then controlled by the collective interactions between the ferroelastic and ferroelectric subsystem.

To summarize, we have explored the effects of AC driving voltage on the measurements local hysteresis loops using PFM. In certain cases, the driving voltage and measurement voltage affect polarization switching equally. The measurements of both field-on and field-off loops then suggest a strategy to elucidate this behavior and distinguish paraelectric materials from ferroelectrics with low coercive biases (for a closed loop V_{ac} gives a top estimate of the coercive bias), as well as from electrostrictive (a V-shaped dependence of PR amplitude on bias in the region of electrostriction). At the same time, for materials with complex domain structures, the field-on and field-off loops contain complementary information on reversible and irreversible polarization dynamics. In all cases, measurements of loop evolution with V_{ac} are a necessary step to establish the veracity of PFM hysteresis measurements.

[1] S. V. Kalinin, A. N. Morozovska, L. Q. Chen, and B. J. Rodriguez, Rep. Prog. Phys. **73**(5), 056502 (2010).

[2] A. Gruverman and A. Kholkin, Rep. Prog. Phys **69**(8), 2443–2474 (2006).

[3] A. Roelofs, U. Bottger, R. Waser, F. Schlaphof, S. Trogisch, and L. M. Eng, Appl. Phys. Lett. **77**(21), 3444–3446 (2000).

[4] M. Alexe, A. Gruverman, C. Harnagea, N. D. Zakharov, A. Pignolet, D. Hesse, and J. F. Scott, Appl. Phys. Lett. **75**(8), 1158–1160 (1999).

[5] B. J. Rodriguez, S. Jesse, A. P. Baddorf, T. Zhao, Y. H. Chu, R. Ramesh, E. A. Eliseev, A. N. Morozovska, and S. V. Kalinin, Nanotechnology **18**(40), 405701 (2007).

[6] D. Guo, I. Stolichnov, and N. Setter, J. Phys. Chem. B **115**(46), 13455–13466 (2011).

[7] S. Jesse, H. N. Lee, and S. V. Kalinin, Rev. Sci. Instrum. **77**(7), 073702 (2006).

[8] N. A. Polomoff, R. N. Premnath, J. L. Bosse, and B. D. Huey, J. Mater. Sci. **44**(19), 5189–5196 (2009).

[9] R. Nath, Y. H. Chu, N. A. Polomoff, R. Ramesh, and B. D. Huey, Appl. Phys. Lett. **93**(7), 072905 (2008).

[10] S. M. Yang, J. Y. Jo, D. J. Kim, H. Sung, T. W. Noh, H. N. Lee, J. G. Yoon, and T. K. Song, Appl. Phys. Lett. **92**(25), 252901 (2008).

[11] D. J. Kim, J. Y. Jo, T. H. Kim, S. M. Yang, B. Chen, Y. S. Kim, and T. W. Noh, Appl. Phys. Lett. **91**(13), 132903 (2007).

[12] C. Dehoff, B. J. Rodriguez, A. I. Kingon, R. J. Nemanich, A. Gruverman, and J. S. Cross, Rev. Sci. Instrum. **76**(2), 023708 (2005).

[13] S. V. Kalinin, S. Jesse, B. J. Rodriguez, Y. H. Chu, R. Ramesh, E. A. Eliseev, and A. N. Morozovska, Phys. Rev. Lett. **100**(15), 155703 (2008).

[14] B. J. Rodriguez, S. Choudhury, Y. H. Chu, A. Bhattacharyya, S. Jesse, K. Seal, A. P. Baddorf, R. Ramesh, L. Q. Chen, and S. V. Kalinin, Adv. Funct. Mater. **19**(13), 2053–2063 (2009).

[15] Y. Wu and M. A. Shannon, Rev. Sci. Instrum. **77**(4), 043711 (2006).

[16] S. V. Kalinin and D. A. Bonnell, Phys. Rev.B **63**(12), 125411 (2001).

[17] H. O. Jacobs, H. F. Knapp, and A. Stemmer, Rev. Sci. Instrum. **70**(3), 1756–1760 (1999).

[18] V. Garcia, S. Fusil, K. Bouzehouane, S. Enouz-Vedrenne, N. D. Mathur, A. Barthelemy, and M. Bibes, Nature **460**(7251), 81–84 (2009).

[19] X. M. Chen, S. Yang, J. H. Kim, H. D. Kim, J. S. Kim, G. Rojas, R. Skomski, H. D. Lu, A. Bhattacharya, T. Santos, N. Guisinger, M. Bode, A. Gruverman, and A. Enders, New J. Phys. **13**, 083037 (2011).

[20] S. Jesse, P. Maksymovych, and S. V. Kalinin, Appl. Phys. Lett. **93**(11), 112903 (2008).

[21] S. Jesse, S. V. Kalinin, R. Proksch, A. P. Baddorf, and B. J. Rodriguez, Nanotechnology **18**(43), 435503 (2007).

[22] W. Lee, H. Han, A. Lotnyk, M. A. Schubert, S. Senz, M. Alexe, D. Hesse, S. Baik, and U. Gosele, Nat. Nanotechnol. **3**(7), 402–407 (2008).

[23] Y. Kim, H. Han, B. J. Rodriguez, I. Vrejoiu, W. Lee, S. Baik, D. Hesse, and M. Alexe, J. Appl. Phys. **108**(4), 042005 (2010).

[24] Y. Kim, A. Kumar, O. Ovchinnikov, S. Jesse, H. Han, D. Pantel, I. Vrejoiu, W. Lee, D. Hesse, M. Alexe, and S. V. Kalinin, ACS Nano **6**(1), 491–500 (2012).

[25] B. D. Huey, C. Ramanujan, M. Bobji, J. Blendell, G. White, R. Szoszkiewicz, and A. Kulik, J. Electroceram. **13**(1–3), 287–291 (2004).

[26] C. Harnagea, M. Alexe, D. Hesse, and A. Pignolet, Appl. Phys. Lett. **83**(2), 338–340 (2003).

[27] S. Jesse, A. P. Baddorf, and S. V. Kalinin, Nanotechnology **17**(6), 1615–1628 (2006).

[28] S. V. Kalinin, S. Jesse, A. Tselev, A. P. Baddorf, and N. Balke, Acs Nano **5**(7), 5683–5691 (2011).

[29] N. Balke, S. Choudhury, S. Jesse, M. Huijben, Y. H. Chu, A. P. Baddorf, L. Q. Chen, R. Ramesh, and S. V. Kalinin, Nat. Nanotechnol. **4**(12), 868–875 (2009).

[30] V. Anbusathaiah, S. Jesse, M. A. Arredondo, F. C. Kartawidjaja, O. S. Ovchinnikov, J. Wang, S. V. Kalinin, and V. Nagarajan, Acta Mater. **58**(16), 5316–5325 (2010).

[31] R. K. Vasudevan, Y. C. Chen, H. H. Tai, N. Balke, P. P. Wu, S. Bhattacharya, L. Q. Chen, Y. H. Chu, I. N. Lin, S. V. Kalinin, and V. Nagarajan, Acs Nano **5**(2), 879–887 (2011).